A Crystalline Supramolecular Polymer Constructed by the Controlled Self-Assembly of Clamparene and Its Application in Photothermal Conversion

Wen-Juan Qu,[a] Wenjing Shi,[a] Ke Wang,[a] Wentao Hu,[a] Hui Sun,[b,c] Qi Lin,[a] Tai-Bao Wei,[a] and Bingbing Shi*[a]

[a]*Key Laboratory of Eco-Functional Polymer Materials of the Ministry of Education, College of Chemistry and Chemical Engineering, Northwest Normal University, Lanzhou 730070, P. R. China.*

[b]*Hangzhou Zhijiang Silicone Chemical Co. Ltd.*

[c]*Zhejiang Provincial Key Laboratory of High-Performance Bonding Functional Materials and Application Technology*

E-mail: bingbingshi@nwnu.edu.cn

Supporting Information (10 Pages)

1. Materials and methods

All reagents were commercially available and used as supplied without further purification. Solvents were either employed as purchased or dried according to procedures described in the literature. Clamparene (**CLP**) was prepared according to our previously reported procedure.[S1]

^{1}H NMR spectra were recorded with a Bruker Avance DMX-400 using the deuterated solvent as the lock and the residual solvent or TMS as the internal reference.

UV-vis spectra were taken on a Shimadzu UV–2550 spectrophotometer. The spectrophotometer used for solid-state UV spectroscopy was Shimadzu UV–2100 spectrometer.

Thermogravimetric Analysis (TGA) analysis was carried out using a Q5000IR analyzer (TA instruments) with an automated vertical overhead thermobalance. The samples were heated at the rate of 10 °C/min using N_2 as the protective gas.

Powder X-ray diffraction (PXRD) data were collected in transmission mode on samples held on thin Mylar film in aluminum well plates on a Panalytical X'Pert PRO MPD equipped with a high throughput screening (HTS) XYZ stage, X-ray focusing mirror, and PIXcel detector, using Ni-filtered Cu Kα radiation.

A xenon lamp (CEL-S500, China) was used to simulate sunlight and the simulated sunlight was allowed to shine in a fixed vertical direction. The calibration of light irradiation intensity was carried out precisely with the utilization of a light radiometer (CEL-FZ-A, China). An infrared thermal imager (Testo 869, China) was utilized to capture variations in the surface temperature of the samples.

Single crystals growth were performed via the following methods:

TCNQ@CLP:

In a 10 mL glass vial, 14.16 mg of dried CLP powder and 2.55 mg of dried TCNQ powder were added with a molar ratio of CLP to TCNQ = 2:1. The mixture was dissolved in a mixed solvent of 5 mL dichloromethane and 1 mL acetonitrile (volume ratio = 5:1). Yellow block-shaped TCNQ@CLP crystals were obtained via slow solvent diffusion at room temperature for 2–3 days.

*2. ^1H NMR studies between **CLP** and **TCNQ** in solution*

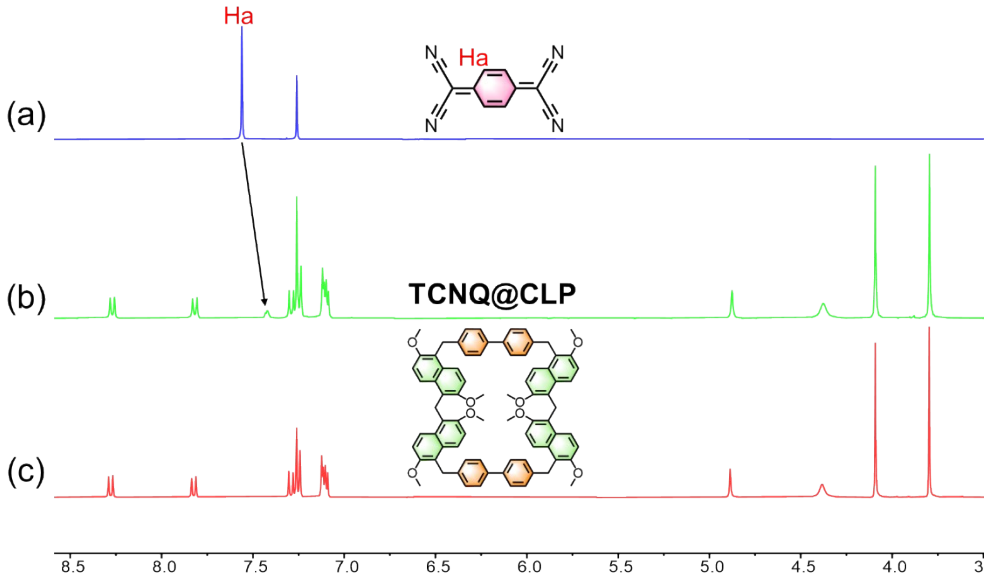

Figure S1. Partial ^1H NMR (400 Hz, $CDCl_3$, 298 K) spectra: (a) **TCNQ** (5.0 mM); (b) **CLP** (10.0 mM) and **TCNQ** (5.0 mM); (c) **CLP** (5.0 mM).

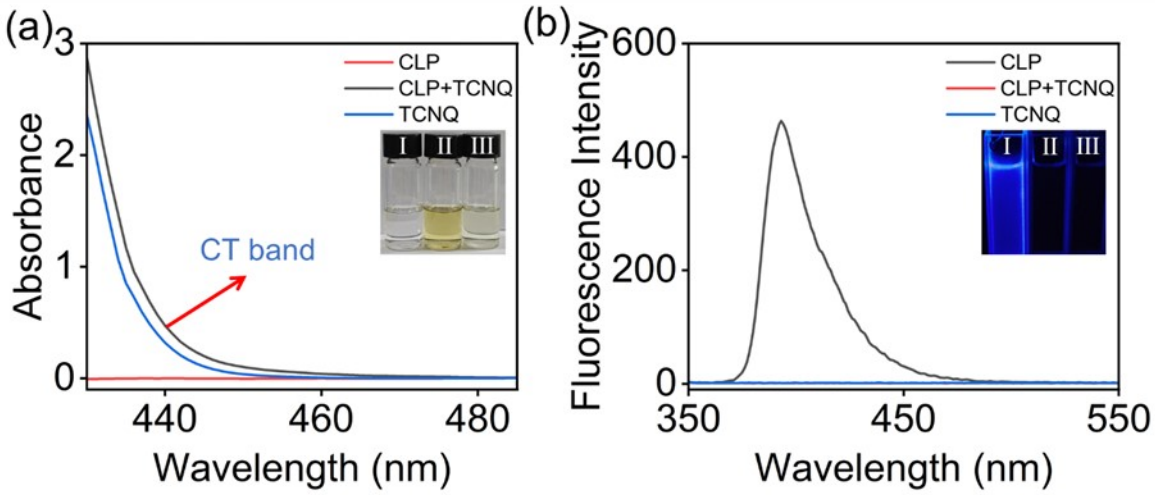

Figure S2. (a) UV-vis spectra (CH_2Cl_2): **CLP** (2.0 mM); **CLP** (2.0 mM) and **TCNQ** (1.0 mM); **TCNQ** (1 mM); inset: photos of the CH_2Cl_2 solution of (I) **CLP**, (II) **CLP** + **TCNQ** and (III) **TCNQ**. (b) Fluorescence spectra (CH_2Cl_2): **CLP** (2.0 mM); **CLP** (2.0 mM) and **TCNQ** (1.0 mM); **TCNQ** (1.0 mM); inset: photos of the CH_2Cl_2 solution of (I) **CLP**, (II) **CLP** + **TCNQ** and (III) **TCNQ**.

*3. Self-assembled single-crystal structure of **CLP** and **TCNQ***

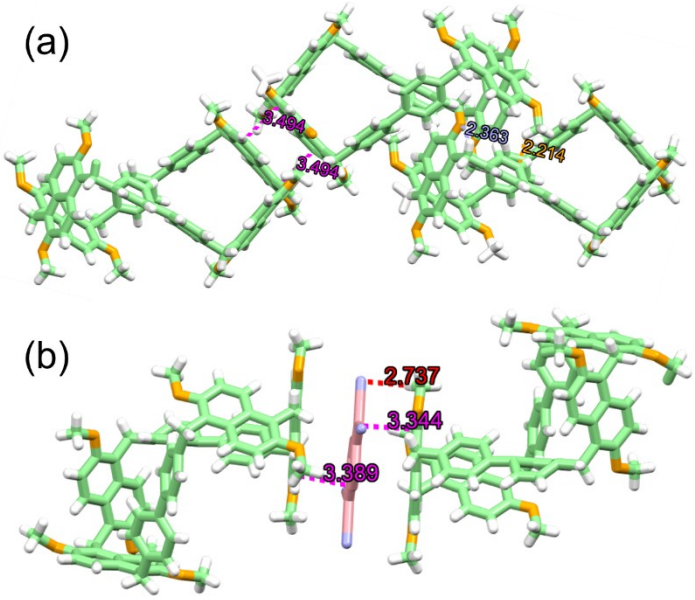

Figure S3. (a) Interactions within the **CLP** itself: purple lines indicate $\pi-\pi$ interactions, orange lines indicate C–H$\cdots\pi$ interactions, while light purple lines initially denote C–H$\cdots$O interactions; (b) Interactions between **CLP** and **TCNQ**: Red lines indicate C–H$\cdots$N interactions, purple lines indicate $\pi-\pi$ interactions.

*4. DFT calculations of **CLP**, **TCNQ@CLP** and **TCNQ***

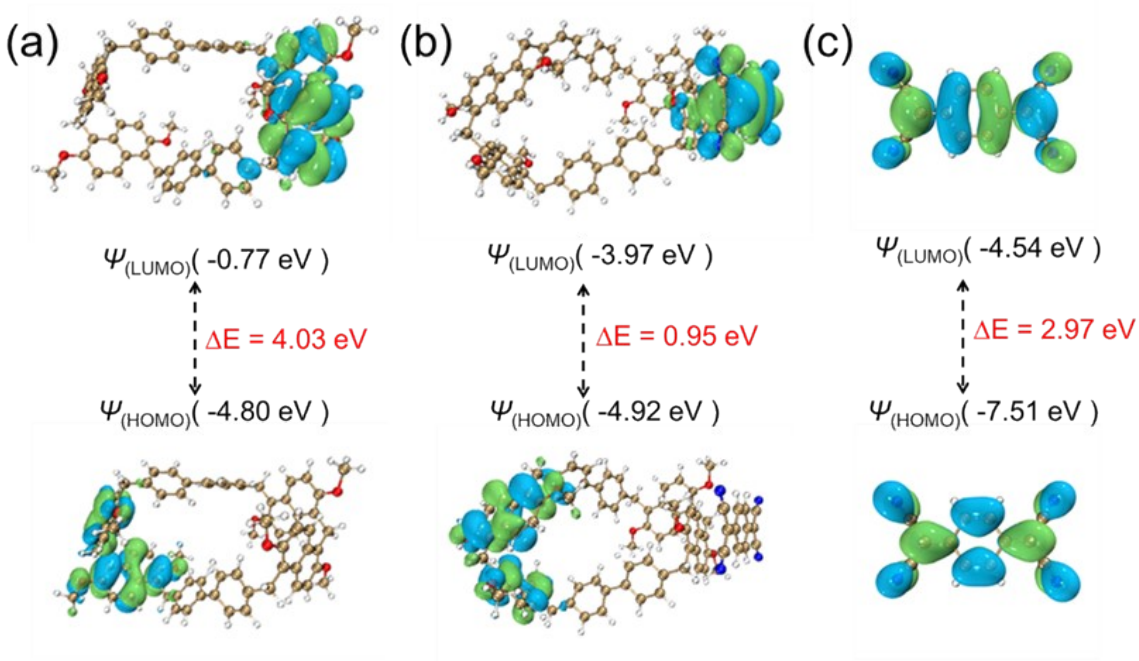

Figure S4. DFT calculations. Frontier molecular orbitals of **CLP**, **TCNQ@CLP** and **TCNQ** and the corresponding first energy gaps (4.03 eV, 0.95 eV and 2.97 eV, respectively).

*5. Study of **2,6-DMN** and **TCNQ** in solution*

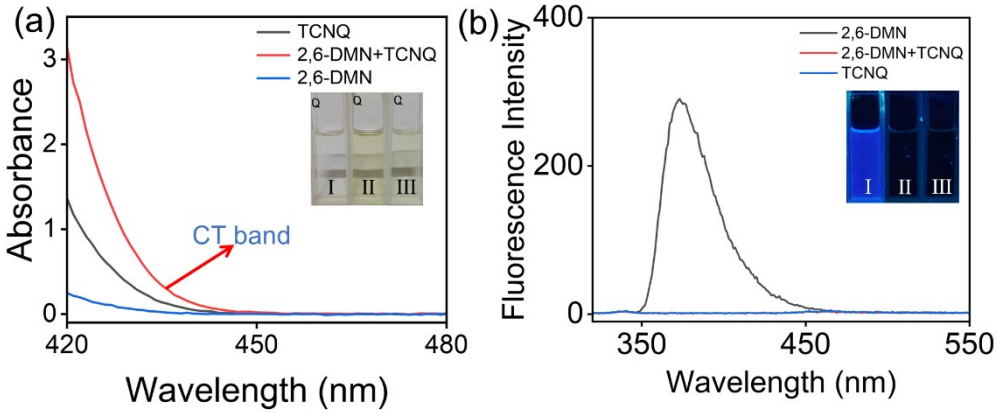

Figure S5. (a) UV-vis spectra (CH_2Cl_2): **2,6-DMN** (2.0 mM); **2,6-DMN** (2.0 mM) and **TCNQ** (1.0 mM); **TCNQ** (1 mM); inset: photos of the CH_2Cl_2 solution of (I) **2,6-DMN**, (II) **2,6-DMN** + **TCNQ** and (III) **2,6-DMN**. (b) Fluorescence spectra (CH_2Cl_2): **2,6-DMN** (2.0 mM); **2,6-DMN** (2.0 mM) and **TCNQ** (1.0 mM); **TCNQ** (1.0 mM); inset: photos of the CH_2Cl_2 solution of (I) **2,6-DMN**, (II) **2,6-DMN** + **TCNQ** and (III) **TCNQ**.

*6. Preparation and Characterization of the Crystalline Supramolecular Polymer **TCNQ@2,6-DMNα***

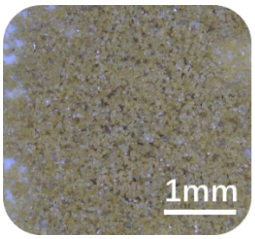

Figure S6. Photographs of **TCNQ@2,6-DMNα**.

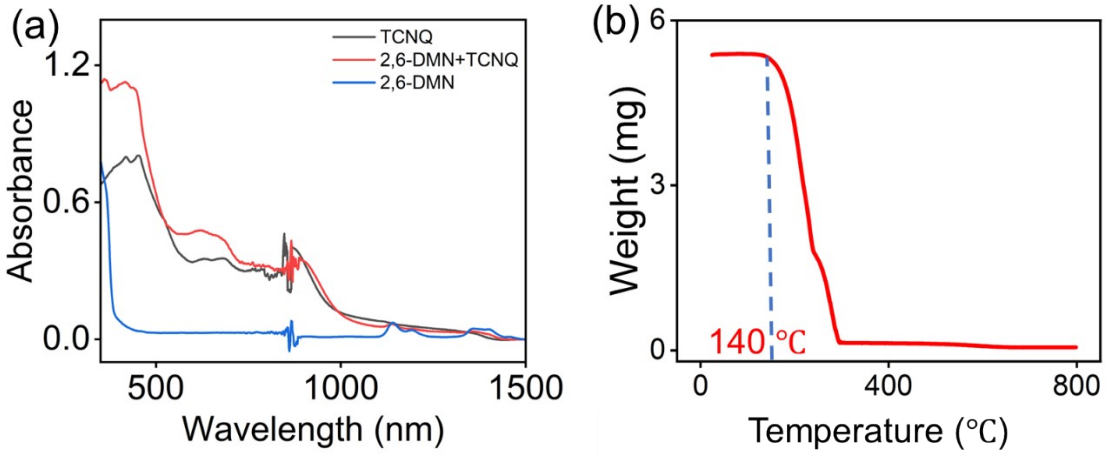

Figure S7. (a) Solid-state UV-vis absorption spectrum of **TCNQ@2,6-DMNα**. (b) Thermogravimetric analysis of **TCNQ@2,6-DMNα**.

7. Photothermal Conversion Studies

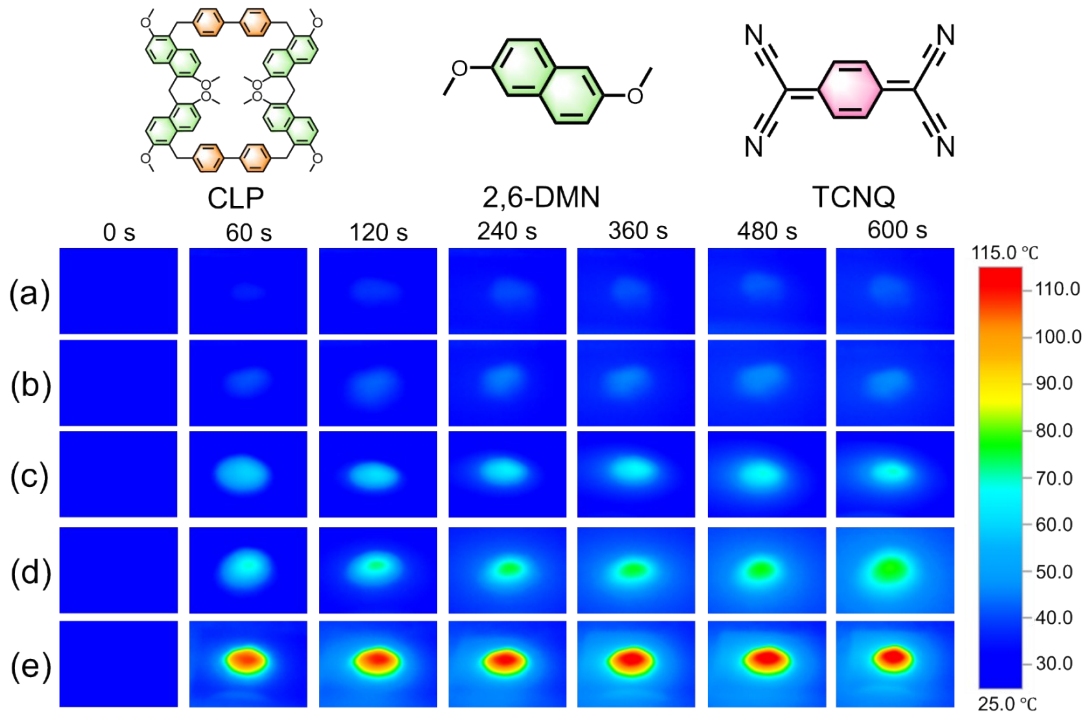

Figure S8. IR camera pictures of (a) **CLP**, (b) **2,6-DMN**, (c) **TCNQ**, (d) **TCNQ@2,6-DMNα** and (e) **TCNQ@CLPα** under 0.35 W·cm^{-2} light irradiation.

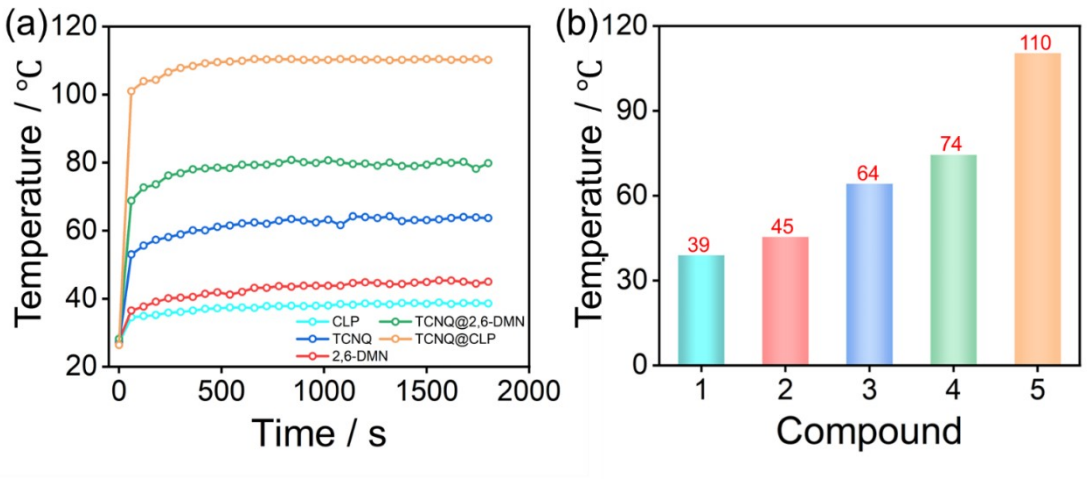

Figure S9. (a) PTC behavior of **CLP**, **2,6-DMN**, **TCNQ**, **TCNQ@2,6-DMNα** and **TCNQ@CLPα** under 0.35 W·cm^{-2}. (b) **CLP**, **2,6-DMN**, **TCNQ**, **TCNQ@2,6-DMNα** and **TCNQ@CLPα** at the maximum temperature under irradiation at 0.35 W·cm^{-2}.

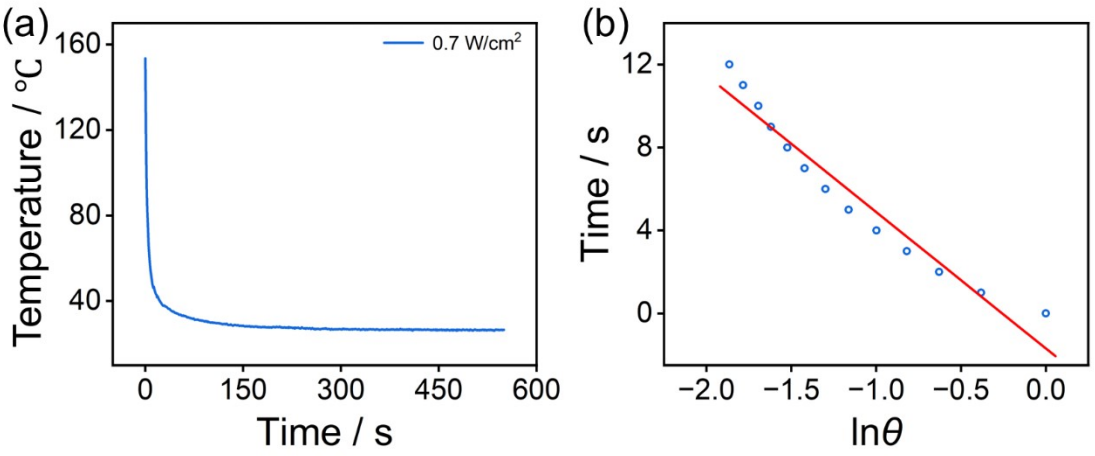

Figure S10. (a) The cooling curve of **TCNQ@CLPα** sample after 808 nm laser irradiation at 0.7 W·cm^{-2}. (b) The corresponding time-lnθ linear curve.

8. Calculation of the photothermal conversion efficiency

The **TCNQ@CLPα** cocrystals were irradiated by NIR laser (808 nm) with a power density of 0.7 W cm^{-2} for 20 min. Then, the system cools naturally and the temperature change is recorded by IR thermal camera. The photothermal conversion efficiency (PCE, η) of **TCNQ@CLPα** cocrystals can be calculated according to the previous method[S2, S3] Details are as follows: Based on the total energy balance for this system:

$$\sum_i m_i C_{p,i} = Q_s - Q_{loss}$$

Where m_i (27.6 mg) and $C_{p,i}$ (1.029 J·g^{-1}·K^{-1}) are the mass and heat capacity of cocrystal samples, respectively. Q_s is the photothermal heat energy input by irradiating NIR laser to cocrystal sample, and Q_{loss} is thermal energy lost to the surroundings. When the temperature is maximum, the system is in balance.

$$Q_s = Q_{loss} = hS\Delta T$$

Where h is heat transfer coefficient, S is the surface area of the samples, $\triangle T_{max}$ is the maximum temperature change. The photothermal conversion efficiency η is calculated from the following equation:

$$\eta = \frac{hS\Delta T_{max}}{I(1 - 10^{-A808})}$$

Where I is the laser power (0.7 W cm^{-2}) and A808 is the absorbance of the samples at the wavelength of 808 nm (1.024).

In order to get the *hS*, a dimensionless driving force temperature, θ is introduced as follows:

$$\theta = \frac{T - T_{surr}}{T_{max} - T_{surr}}$$

Where T is the temperature of cocrystal, Tmax is the maximum system temperature (160.4 °C), and Tsurr is the initial temperature (28.2 °C). And a sample system time constant τ_s

$$\tau_s = \frac{\sum_i m_i C_{p,i}}{hS}$$

Thus, $$\frac{d\theta}{dt} = \frac{1 \quad Q_s}{\tau_s hS \Delta T_{max}} - \frac{\theta}{\tau_s}$$

When the laser is off, $Q_S = 0$, therefore $\frac{d\theta}{dt} = -\frac{\theta}{\tau_s}$, and $t = -\tau_s \ln \theta$.

So *hS* could be calculated from the slope of cooling time vs Inθ. Therefore, τ_s is 6.58 s (Figure S7b). And the photothermal conversion efficiency η is 90.03 %.

9. X-ray Crystallographic data

*Crystal Structure Determinatio*n: Single-crystal X-ray diffraction data was collected on a Nonius Kappa CCD diffractometer and a BRUKER APEXII CCD. The APEX3 software suite was used to manage data collection, reduction (SAINT V8.38A1), absorption correction by the Multi-scan method (SADABS), structure determination via direct methods (SHLEXT) and model refinement (SHELXL). All non-hydrogen atoms were refined anisotropically and all hydrogen atoms were refined with isotropically with their positions constrained to their carriers. Platon Squeeze was used to account for regions of heavily disordered solvent that could not be modlled. Supplementary CIFs, which include structure factors, are available free of charge from the Cambridge Crystallographic Data Centre (CCDC) via www.ccdc.cam.ac.uk/data_request/cif.

Table S1 Crystallographic data of **TCNQ@CLP**.

Empirical formula	$C_{97}H_{89.5}N_{8.5}O_8$
Formula weight	1502.27
Temperature/K	150.00(10)
Crystal system	triclinic
Space group	P-1
a/Å	13.7704(3)
b/Å	14.3626(3)
c/Å	23.1211(4)
α/°	100.012(2)
β/°	99.963(2)
γ/°	110.512(2)
Volume/Å^3	4079.80(15)
Z	2
ρ_{calc}g/cm^3	1.223
μ/mm^{-1}	0.622
F(000)	1590.0
Crystal size/mm^3	0.1 × 0.07 × 0.06
Radiation	Cu Kα (λ = 1.54184)
2Θ range for data collection/°	6.794 to 155.014
Index ranges	-17 ≤ h ≤ 17, -17 ≤ k ≤ 18, -29 ≤ l ≤ 19
Reflections collected	58351
Independent reflections	16404 [R_{int} = 0.0357, R_{sigma} = 0.0354]
Data/restraints/parameters	16404/2279/1477
Goodness-of-fit on F^2	1.048
Final R indexes [I>=2σ (I)]	R_1 = 0.0880, wR_2 = 0.2637
Final R indexes [all data]	R_1 = 0.1100, wR_2 = 0.2831
Largest diff. peak/hole / e Å^{-3}	0.67/-0.33

CCDC	2519019

10. References:

S1. Shi, B.; Jiang, J.; An, H.; Qi, L. J.; Wei, T.-B.; Qu, W.-J.; Lin, Q. Clamparene: Synthesis, Structure, and Its Application in Spontaneous Formation of 3D Porous Crystals. *J. Am. Chem. Soc.* **2024**, *146*, 2901–2906.

S2. Zhao, Y.; Chen, J.; Su, Y.; Cao, Y.; Wu, B.; Yu, S.; Li, M.-D.; Wang, Z.; Zheng, M.; Zhuo, M.-P.; Liao, L.-S. Organic Charge-Transfer Cocrystals toward Large-Area Nanofiber Membrane for Photothermal Conversion and Imaging. *ACS Nano* **2022**, *16*, 15000.

S3. Wang, R.; Su, Y.; Xiao, Z.; Wang, T.; Liu, K.; Gong, Z.; Wu, J.; Chen, J.; Liu, Z.; Li, B.; Zhang, X.; Li, C.; et al. Ternary Inclusion Co-Crystals for Efficient Photothermal Conversion and Solar-Driven Water Evaporation. *Adv. Sci.* **2025**, *12*, 2500050.